Complex-valued belief divergence measure and its application on information fusion

Mengzhuo Zhang[1], Yifan Sun[1], Xiaozhuan Gao[1*†], Lipeng Pan[1,2,3*†]

[1]College of Information Engineering, Northwest A&F University, Yangling, Xianyang, 712100, Shaanxi, China.
[2]Shaanxi Engineering Research Center for Intelligent Perception and Analysis of Agricultural Information, Northwest A&F University, Yangling, Xianyang, 712100, Shaanxi, China.
[3]Northwest A&F University ShenZhen Research Institute, Northwest A&F University, Shenzhen, 518000, China.

*Corresponding author(s). E-mail(s): gaoxiaozhuan@nwafu.edu.cn; lipeng.pan@nwafu.edu.cn;
Contributing authors: zhangmz@nwafu.edu.cn; 1fan.sun@nwafu.edu.cn;
†These authors contributed equally to this work.

Abstract

In the domain of multi-sensor data fusion, effectively handling and modeling uncertainty of information can improve information quality, thereby improving the accuracy of the fusion results. Dempster-Shafer(D-S) evidence theory offers a powerful approach due to its adaptability and potency in handling and modeling the indeterminate information. Nevertheless, due to its reliability hypothesis, further applications are limited, which reduces the accuracy of the fusion results. To address this issue, complex-valued evidence theory uses phase angle and amplitude to model random information and reliability information. But it is worth studying how to measure the difference between two mass functions, as it can boost the precision of the fusion results. This paper introduces an innovative complex-valued belief divergence that considers the influence of phase angle to measure the difference of information. Additionally, we designed an information fusion model based on the proposed divergence and it can be verified by some real-world datasets.

Keywords: Dempster-Shafer evidence theory, Complex-valued evidence theory, Belief Jensen-Shannon divergence, Belief entropy

1 Introduction

Data fusion is crucial in practical applications, including disaster emergency management[1, 2], intelligent fault diagnosis[3], medical data processing[4], image manipulation[5], object tracking[6], and so on[7, 8]. How to model and express uncertain information is crucial for improving the accuracy of fusion system results[9]. There are some method proposed to handle it, such as Bayesian probability[10], rough sets[11], fuzzy sets[12], D-S evidence theory[13, 14], random permutation[15] and more extensions[16, 17]. Those methods have received widespread attention and have been implemented across diverse domains, including object recognition and classification, information fusion, decision-making etc[18–21]. In those methods, D-S evidence theory is increasingly recognized for its adaptability and potency in modeling and processing the indeterminate information[22, 23]. The D-S evidence theory, by assigning basic probability among power set of events, can simultaneously model unknown and uncertain information, so it has more strong uncertain representation ability than probability[24, 25]. Besides, Dempster's combination rule enables the synthesis different pieces of evidence by computing the conflict among them[26, 27]. Because these advantages, it has received widespread attention and application[28–31].

Recently, some studies have expanded expression of uncertain information from real plane to complex plane to improve the accuracy of the results, such as probability theory and fuzzy theory[32–34]. Ramot et al use unit circle within the complex plane to model membership function, which is interpretable through solar activity (as indicated by sunspot count measurements), and is applicable in the context of signal processing[35]. Garg and Rani[36] use complex intuitionistic fuzzy set to model imprecision and ambiguity in the data, based on it, they propose some aggregation operators that are used in multi-criteria decision-making problem. Similarly, some scholars have also explored the expression and modeling of the D-S evidence theory in the field of complex numbers. Xiao et al[37, 38] express uncertain information within the quantum framework of Hilbert space and explore some related operations that are used in pattern classification and decision-making. The mathematical framework of D-S evidence theory operates under the reliability hypothesis. To break through reliability hypothesis, Pan and Deng proposed complex-value evidence theory (CVET) to model reliability information, which have been widely validated and applied[17, 39].

Although CVET provides a feasible method to model the reliability of information using phase angles in complex numbers. However, how to establish divergence measurement in complex-valued space and further effectively measure the difference between different information is still a problem that needs to be considered. Jensen-Shannon divergence provides a quantitative way to assess the disparity between two probability assignments[40]. A smaller divergence value indicates that the two distributions are more similar, while a larger value indicates a greater difference, which has been used in many fields[41–43]. ICVET, we not only need to consider the difference between two information distributions, but also the phase angle related to reliability information. Therefore, we introduce a novel method termed the complex-valued belief Jensen-Shannon divergence (CVBJ-SD) to measure difference between information. When the information is completely reliable, CVBJ-SD degenerates into belief Jensen-Shannon divergence which considers difference of amplitude and phase angle.

In addition, it satisfies some general divergence properties, such as non-negativity, reflexivity, symmetry, and so on. To further evaluate the effectiveness of CVBJ-SD, this paper proposes an information fusion model based on CVBJ-SD and applies it to some real-world datasets.

The remaining structure of this article is as follows. Chapter 2 describes the basic knowledge of relevant information. Chapter 3 proposes a new divergence measure under evidence theory, with numerical examples to elucidate its practical application. Chapter 4 applies this measure to an information fusion model, corroborated by real world data. Chapter 5 gives a conclusion.

2 Preliminaries

This section introduces the basic concepts of D-S evidence theory. Furthermore, this section will also cover the concepts of belief entropy and belief divergence measure, which are key metrics for assessing the uncertainty of evidences.

2.1 D-S evidence theory

D-S evidence theory allocates random information to the power set of the framework of discernment(FoD)[13, 14]. This approach can better model and express imprecise information[28]. In this section, we will present the concepts of FoD, mass function(MF), complex-valued mass function(CVMF)[17] and Dempster's combination rule(DCR).

Definition 1 (Frame of discernment)**.** *FoD is composed of some mutually exclusive elements X_i, as shown below.*

$$\Theta = \{X_1, X_2, \cdots, X_i, \cdots, X_N\} \tag{1}$$

Its power set 2^Θ is as follows:

$$2^\Theta = \{\emptyset, \{X_1\}, \cdots, \{X_N\}, \{X_1, X_2\}, \cdots \{X_1, X_2, X_i\}, \cdots, \Theta\}. \tag{2}$$

Let A be an element of 2^Θ and A not be an empty set, where A is referred to as a proposition.

Definition 2 (Mass function)**.** *For a FoD Θ , the mass function $m : 2^\Theta \to [0, 1]$,the following conditions are satisfied:*

$$\begin{cases} m(\emptyset) = 0, \\ \sum_{A \in 2^\Theta} m(A) = 1. \end{cases} \tag{3}$$

The $m(A)$ represents the degree to which evidence body supports the proposition A. If $m(A)$ exceeds zero, A is termed a focal element.

Definition 3 (Complex-valued mass function)**.** *The complex-valued mass function CM is an extension of MF, which assigns complex numbers to each proposition A. the*

following conditions are satisfied:

$$\begin{cases} |CM| : 2^{\Theta} \to [0,1], \\ CM(\emptyset) = 0, \\ CM(A) = M(A)e^{i\pi\theta_A} = x_A + iy_A. \end{cases} \tag{4}$$

where $M(A)$ is the amplitude of $CM(A)$ and satisfied the following equation:

$$\sum_{A\in 2^{\Theta}} M(A) = \sum_{A\in 2^{\Theta}} \sqrt{x_A^2 + y_A^2} = 1 \tag{5}$$

$|CM|$ is the modulus of CM, equivalent to $M(A)$. $M(A)$ indicates the degree to which evidence body supports the proposition A. θ_A is the phase angle of CM, which carries different meanings in various applications. In this paper, θ_A is indicated the reliability of the degree of support for proposition A. Consequently, θ_A is confined within the interval $\left[0, \frac{1}{2}\right]$. When θ_A equals zero, CVMF degenerates into a MF.

Definition 4 (Dempster's combination rule)**.** *Dempster's combination rule is a method used to merge two mass functions(MFs), denoted as m_1 and m_2, on a FoD Θ. The DCR is mathematically expressed as $m = m_1 \bigoplus m_2$. It uses the following equation to combine m_1 and m_2 into a new function m:*

$$m(A) = \begin{cases} 0 & A = \emptyset \\ \frac{1}{1-K} \sum_{B\cap C=A} m_1(B)m_2(C) & A \neq \emptyset \end{cases} \tag{6}$$

with

$$K = \sum_{B\cap C=\emptyset} m_1(B)m_2(C). \tag{7}$$

Both B and C are elements of the power set 2^{Θ}. K is utilized to measure the level of conflict between two MFs. The larger the K, the greater the level of conflict. The rule is only applicable when the value of K is less than 1.

2.2 Belief entropy

In the D-S evidence theory, Shannon entropy is not a suitable metric for quantifying the uncertainty of MFs, as it does not account for effect of the count of focal elements on the level of uncertainty. To address this, Deng introduced Deng entropy, also referred to as belief entropy, to quantify the MF's uncertainty. The higher the belief entropy, the greater the level of uncertainty. Similarly, Pan and Deng proposed complex-valued belief entropy to quantify the uncertainty of complex-valued mass function[44].

Definition 5 (Belief entropy)**.** *Belief entropy is an uncertainty measure specifically designed for the mass function, is formulated as:*

$$E_d = -\sum_{A\in 2^{\Theta}} m(A) \log \frac{m(A)}{2^{|A|} - 1}, \tag{8}$$

Definition 6 (Complex-valued belief entropy)**.** *The uncertainty of the CVMF can be quantified using complex-valued belief entropy. The definition of complex-valued belief entropy is presented below:*

$$CE_d = \left| -\sum_{A \in 2^\Theta} \left| M(A) e^{i\pi\theta_A} \right| \log \frac{M(A) e^{i\pi\theta_A}}{2^{|A|} - 1} \right|, \tag{9}$$

Where $\left| M(A) e^{i\pi\theta_A} \right|$ *is the modulus of* $M(A) e^{i\pi\theta_A}$*, equivalent to* $M(A)$*. Based on the properties of logarithmic function, we can transform the above equation as follows:*

$$CE_d = \left| -\sum_{A \in 2^\Theta} \Big(M(A) \log M(A) + M(A) \log e^{i\pi\theta_A} - M(A) \log(2^{|A|} - 1) \Big) \right|, \tag{10}$$

Next, we proceed to simplify the expression as follows:

$$CE_d = \left| -\sum_{A \in 2^\Theta} \Big(M(A) \log M(A) + M(A) i\pi\theta_A - M(A) log(2^{|A|} - 1) \Big) \right|. \tag{11}$$

When $\theta_A = 0$, complex-valued belief entropy degenerates into belief entropy. Furthermore, complex-valued belief entropy also satisfies probability consistency and conditions. It is intuitively observable that, as the count of focal elements increases, the complex-valued belief entropy increases correspondingly.

2.3 Belief divergence measure

Divergence is an effective measure for quantifying the discrepancy between information, and it has been extensively utilized in various applications[42]. Based on D-S evidence theory, Xiao proposed belief J-S divergence, which incorporates intrinsic information involved in MF[45].

Definition 7 (Belief Jensen–Shannon divergence)**.** *The belief J–S divergence is used to quantify the discrepancy between two MFs* m_1 *and* m_2*[45]. The formula for its computation is given by:*

$$BJS(m_1, m_2) = \frac{1}{2} \left[S\left(m_1, \frac{m_1 + m_2}{2} \right) + S\left(m_2, \frac{m_1 + m_2}{2} \right) \right], \tag{12}$$

with $S(m_1, m_2) = \sum_{A \subseteq 2^\Theta} m_1(A) \log \frac{m_1(A)}{m_2(A)}$ *represents the Kullback-Leibler(KL) divergence, with* $\sum_{A \subseteq 2^\Theta} m_j(A) = 1 (j = 1, 2)$ *being satisfied.*

When the mass function is zero, it becomes apparent that the ratio approaches infinity, and consequently, the logarithm of this ratio will also tend towards infinity. In such circumstances, the previously proposed method becomes ineffective. Therefore, we use a very small number 1×10^{-12} to replace zero value when such a scenario arises.

3 Complex-valued belief divergence measure

Although divergence is an effective measure for quantifying the discrepancy between information[46, 47], existing methods have not fully utilized the phase angle information to construct divergence models. Therefore, we introduce a novel divergence named Complex-valued belief Jensen-Shannon divergence (CVBJ-SD) to quantify the discrepancy between information within complex-valued space.

Definition 8 (Complex-valued Kullback-Leibler divergence)**.** *Let CM_1 and CM_2 be two CVMFs on the FoD Θ. The Complex-valued Kullback-Leibler divergence $S(CM_1, CM_2)$ is defined as follows:*

$$S(CM_1, CM_2) = \sum_{A \subseteq 2^\Theta} \left[\|CM_1(A)\| \log \frac{M_1(A)}{M_2(A)} + \|CM_1(A)\| \log \frac{e^{i\theta_1(A)}}{e^{i\theta_2(A)}} \right]. \tag{13}$$

According to the properties of logarithmic functions, it can be simplified as follows:

$$S(CM_1, CM_2) = \sum_{A \subseteq 2^\Theta} \left[M_1(A) \log \frac{M_1(A)}{M_2(A)} + M_1(A)|\theta_1(A) - \theta_2(A)|i \right]. \tag{14}$$

The Complex-valued KL divergence quantifies the discrepancy between two complex-valued mass functions. However, KL divergence is asymmetric, which may lead to misunderstandings regarding model performance. Consequently, we introduce a novel measure, the CVBJ-SD, which is based on the KL divergence and addresses its asymmetry issue.

Definition 9 (Complex-valued belief Jensen-Shannon divergence)**.** *The CVBJ-SD between CM_1 and CM_2 is defined as follows:*

$$CVBJ - SD(CM_1, CM_2) = \sqrt{\left| \left| \frac{1}{2} \left[S\left(CM_1, \frac{CM_1 + CM_2}{2}\right) + S\left(CM_2, \frac{CM_1 + CM_2}{2}\right) \right] \right|} \tag{15}$$

It can effectively measure the discrepancy by simultaneously taking into account both amplitude and phase angle in complex space. When the phase angle is 0, it degenerates into real space. In addition, CVBJ-SD possesses several general properties, including non-negativity, symmetry, reflexivity and transitivity. Below, we will prove these four properties.

(1)Non-Negativity: $CVBJ - SD(CM_1, CM_2) \geq 0$.

Clearly, for any two MFs CM_1 and CM_2,the result of calculating $S(CM_1, CM_2)$ is a complex number. Consequently, it follows that the result of $\frac{1}{2}\left[S\left(CM_1, \frac{CM_1+CM_2}{2}\right) + S\left(CM_2, \frac{CM_1+CM_2}{2}\right)\right]$ is also complex number. The modulus of this complex number is a non-negative real number. Its square root is also a non-negative real number. So, CVBJ-SD satisfies non-negativity.

(2)Symmetry: $CVBJ - SD(CM_1, CM_2) = CVBJ - SD(CM_2, CM_1)$.

Consider two mass functions CM_1 and CM_2:

$$CVBJ-SD(CM_2,CM_1)=\sqrt{\left|\left|\frac{1}{2}\left[S\left(CM_2,\frac{CM_2+CM_1}{2}\right)+S\left(CM_1,\frac{CM_2+CM_1}{2}\right)\right]\right|\right|}.$$

According to the additive commutative law, we can directly conclude that $CVBJ-SD(CM_1,CM_2)=CVBJ-SD(CM_2,CM_1)$. Therefore, CVBJ-SD satisfies symmetry.

(3)Reflexivity: $CVBJ-SD(CM_1,CM_2)=0$ when $CM_1=CM_2$,.

When $CM_1=CM$ and $CM_2=CM$, it follows that $\frac{CM_1+CM_2}{2}=CM$. Given this, the Complex-valued Kullback-Leibler divergence $S(CM,CM)$ is:

$$S(CM,CM)=\sum_{A\subseteq 2^{\Theta}}\left[M(A)\log\frac{M(A)}{M(A)}+M(A)|\theta(A)-\theta(A)|i\right]=0.$$

The $CVBJ-SD(CM_1,CM_2)$ simplifies to:

$$\begin{aligned}CVBJ-SD(CM_1,CM_2)&=\sqrt{\left|\left|\frac{1}{2}\left[S\left(CM_1,\frac{CM_1+CM_2}{2}\right)+S\left(CM_2,\frac{CM_1+CM_2}{2}\right)\right]\right|\right|}\\&=\sqrt{\left|\left|\frac{1}{2}\left[S\left(CM,CM\right)+S\left(CM,CM\right)\right]\right|\right|}\\&=0.\end{aligned}$$

Thus, CVBJ-SD satisfies reflexivity.

(4)Transitivity: If $CVBJ-SD(CM_1,CM_2)=0$ and $CVBJ-SD(CM_1,CM_3)=0$, then
$CVBJ-SD(CM_2,CM_3)=0$.

,When the value of CVBJ-SD is zero, it indicates that two MFs are the same. Therefore, we have $CM_1=CM_2$ and $CM_1=CM_3$. So there is $CM_2=CM_3$, we can infer that $CVBJ-SD(CM_2,CM_3)=0$. Thus, CVBJ-SD satisfies transitivity.

We have provided a detailed proof of the properties of CVBJ-SD above. Next, we will give several specific examples to illustrate how it can be applied.

Example 3.1 Assuming there are two complex-valued mass functions, denoted as CM_1 and CM_2, defined within the frame of discernment $\Theta=\{X_1,X_2\}$, these two functions are specified as follows:

$$CM_1:CM_1(X_1)=0.3e^{0.3\pi i},CM_1(X_2)=0.7e^{0.25\pi i}.$$

$$CM_2:CM_2(X_1)=0.8e^{0.2\pi i},CM_2(X_2)=0.2e^{0.4\pi i}.$$

The Complex Belief Jensen–Shannon divergence between CM_1 and CM_2 $CVBJ-SD(CM_1,CM_2)$ was calculated as follows:

Step 1 Calculate the average of CM_1 and CM_2:

Supposing $CM_3 = \frac{CM_1+CM_2}{2}$, CM_3 is calculated as follows:

$$CM_3 : CM_3(X_1) = 0.54e^{0.23\pi i}, CM_3(X_2) = 0.44e^{0.28\pi i}.$$

Step 2 Put the above into the measure:

$$\begin{aligned} S(CM_1, CM_3) &= \sum_j \left[M_1(A_j) * \log \frac{M_1(A_j)}{M_3(A_j)} + M_1(A_j) * |\theta_1 - \theta_3| i\pi \right] \\ &= 0.3 * \log \frac{0.3}{0.54} + 0.3 * |0.3 - 0.23|\, i + 0.7 * \log \frac{0.7}{0.44} + 0.7 * |0.25 - 0.28|\, i \\ &= 0.15 + 0.04i \end{aligned}$$

$$\begin{aligned} S(CM_2, CM_3) &= \sum_j \left[M_2(A_j) * \log \frac{M_2(A_j)}{M_3(A_j)} + M_2(A_j) * |\theta_2 - \theta_3| i\pi \right] \\ &= 0.8 * \log \frac{0.8}{0.54} + 0.8 * |0.2 - 0.23|\, i + 0.2 * \log \frac{0.2}{0.44} + 0.2 * |0.4 - 0.28|\, i \\ &= 0.16 + 0.05i \end{aligned}$$

$$\begin{aligned} CVBJ - SD(CM_1, CM_2) &= \sqrt{\left|\left| \frac{1}{2} * [S(CM_1, CM_3) + S(CM_2, CM_3]) \right|\right|} \\ &= \sqrt{\left|\left| \frac{1}{2} [0.15 + 0.04i + 0.16 + 0.05i] \right|\right|} \\ &= 0.4 \end{aligned}$$

We firstly calculate the average CM_3 of CM_1 and CM_2, Then, $S(CM_1, CM_3)$ and $S(CM_2, CM_3)$ were calculated separately. Finally, substitute it into the Equation 15 to obtain $CVBJ - SD(CM_1, CM_2)$. That is the calculation of CVBJ-SD.

Example 3.2 The CM_1 and CM_2 are given as follows:

$$CM_1 : CM_1(X_1) = 0.7e^{0.25\pi i}, CM_1(X_2) = 0.3e^{0.3\pi i}.$$

$$CM_2 : CM_2(X_1) = 0.8e^{0.2\pi i}, CM_2(X_2) = 0.2e^{0.4\pi i}.$$

The calculation shows that $CVBJ - SD(CM_1, CM_2)$ is as follows:

$$CM_3 : CM_3(X_1) = 0.75e^{0.22\pi i}, CM_3(X_2) = 0.25e^{0.34\pi i}.$$

$$CVBJ-SD(CM_1,CM_2)=\sqrt{\left|\left|\frac{1}{2}*S\left(CM_1,CM_3\right)+\frac{1}{2}*S\left(CM_2,CM_3\right)\right|\right|}=0.18.$$

By analyzing these two examples, we can conclude the following: In Example 3.1, CM_1 has a higher degree of support for proposition X_2, while CM_2 is the opposite. In Example 3.2, both CM_1 and CM_2 exhibit a higher degree of support for proposition $_1$. Consequently, the difference in the mass functions' support in Example 3.1 are more pronounced, which is reflected in the calculation results of their CVBJ-SD, that is, the divergence value of Example 3.1 is greater than that of Example 3.2, consistent with our expected analysis.

Example 3.3 The CM_1 and CM_2 are given as follows:

$$CM_1:CM_1(_1)=\frac{\sqrt{x^2+y^2}}{\sqrt{x^2+y^2}+\sqrt{(1-x)^2+y^2}}e^{i\arctan\frac{y}{x}},$$
$$CM_1(_2)=\frac{\sqrt{(1-x)^2+y^2}}{\sqrt{x^2+y^2}+\sqrt{(1-x)^2+y^2}}e^{i\arctan\frac{y}{1-x}}.$$

$$CM_2:CM_2(_1)=\frac{\sqrt{(1-x)^2+y^2}}{\sqrt{x^2+y^2}+\sqrt{(1-x)^2+y^2}}e^{i\arctan\frac{y}{1-x}},$$
$$CM_2(_2)=\frac{\sqrt{x^2+y^2}}{\sqrt{x^2+y^2}+\sqrt{(1-x)^2+y^2}}e^{i\arctan\frac{y}{x}}.$$

Both x and y fall within the interval [0,1], so we can infer that the values of arctan $\frac{y}{x}$ and arctan $\frac{y}{1-x}$ are within the range of $[0,\frac{\pi}{2}]$, which is consistent with our definition of phase angle.

This example will visually demonstrate the impact of amplitude and phase angle on CVBJ-SD. The range of x is between [0,1], and the range of y is between $[0,\frac{\pi}{2}]$. The change of CVBJ-SD is shown in Figure 1. It can be seen that when x=0.5, the divergence value is always 0. At this moment, CM_1 and CM_2 are completely equal, therefore, the divergence is 0. The above results verify the rationality of the model.

Figure 2 presents a heat map of the values of CVBJ-SD. Brighter colors on the map indicate larger CVBJ-SD values. It can be seen that CVBJ-SD value is symmetric about the line x=0.5 and reaches its maximum value when y=0 and x=0 or 1. Figure 3 illustrates the variation of CVBJ-SD as the parameter x changes. It can be more clearly seen that CVBJ-SD value satisfies symmetry and $0\leq CVBJ-SD(CM_1,CM_2)\leq 1$. Figure 4 illustrates the variation of CVBJ-SD as the parameter y changes. As the value of the parameter y increases from 0 to 1, CVBJ-SD value shows an overall downward trend.

4 Application in information fusion

Information fusion can effectively integrate data from multiple sources to obtain more comprehensive and accurate information[48]. To further explain the effectiveness of

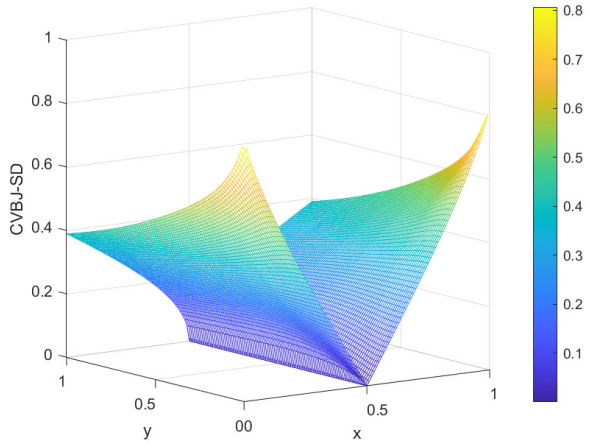

Fig. 1 Three-dimensional map of the CVBJ-SD values

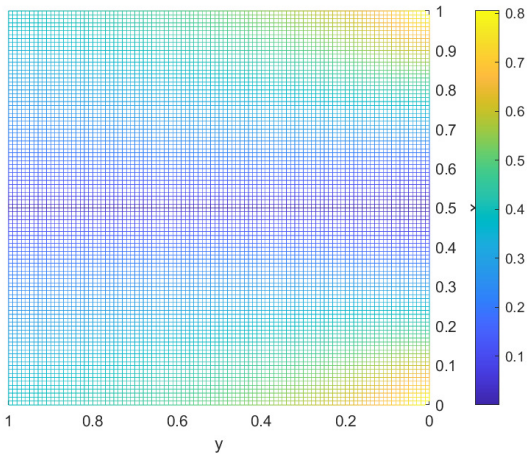

Fig. 2 Heatmap map of the CVBJ-SD values

CVBJ-SD, this part designs an innovative approach to information fusion utilized CVBJ-SD which can be demonstrated by some real world datasets. New model aims to improve the accuracy of decision systems by quantifying the difference between information.

4.1 Information fusion model based on CVBJ-SD

New information fusion model mainly includes the following steps: genertaion of complex-valued mass function, information fusion based on CVBJ-SD and decision-making. Besides, Iris dataset can be used to better explain the new model.

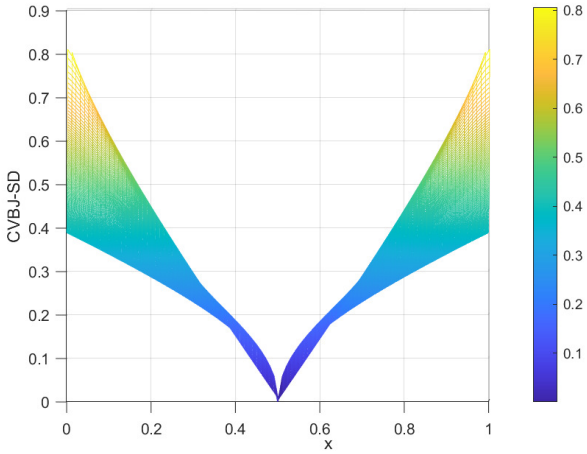

Fig. 3 CVBJ-SD under variations in x

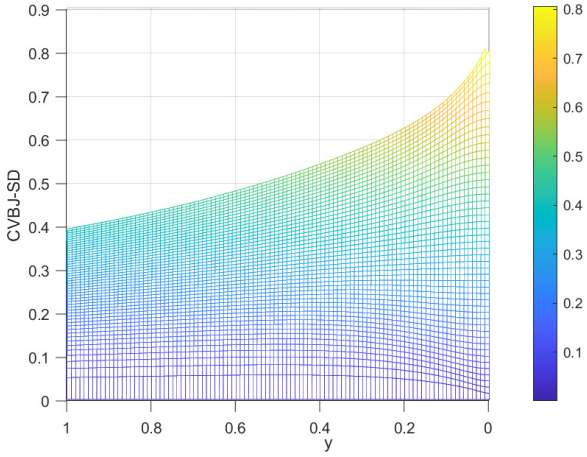

Fig. 4 CVBJ-SD under variations in y

4.1.1 Method for generating complex-valued mass function

We use the idea of marginal contribution to design a method for generating CVMF[17]. Iris dataset has three class, namely Setosa(Se), Versicolor(Ve) and Virginica(Vi). Each class contains four attributes, namely, sepal length (SL), sepal width (SW), petal length (PL) and petal width (PW). In Iris dataset, the framework of discernment is defined as $\{Se, Ve, Vi\}$. In Iris dataset, there is four attributes so every test data would genetate fours complex-valued mass functions. Algorithm 1 provides pseudo-code for generating complex-valued mass function.

In algorithm 1, all propositions in the event space corresponding to the focal element assigned by the complex-valued mass function, namely

Algorithm 1 The generation method of the complex-valued mass function

Require: Training set and test set

Ensure: Complex-valued mass function

for $k = 1$ to 4 **do**
  for $p = 1$ to 7 **do**
    calculate $\delta_{F_p}^k, \mu_{F_p}^k, \delta_{F_p'}^k, \mu_{F_p'}^k$;
    $\Delta\delta_{F_p}^k = |\delta_{F_p'}^k - \delta_{F_p}^k|, \Delta\mu_{F_p}^k = |\mu_{F_p'}^k - \mu_{F_p}^k|$;
    if $\Delta\mu_{F_p}^k > \frac{\pi}{2}$ **then**
      Set $\Delta\mu_{F_p}^k = \frac{\pi}{2}$;
    end if
    $CM_k^o(F_p) = \left(\frac{1}{e^{\Delta\mu_{F_p}^k}}\right) e^{i\left(\Delta\delta_{F_p}^k\right)}$;
  end for
  Normalize the CM_k^o to give the CM_k
end for

$\{\{Se\}, \{Ve\}, \{Vi\}, \{Se, Ve\}, \{Se, Vi\}, \{Ve, Vi\}, \{Se, Ve, Vi\}\}$, also named as $\{\{F_1\}, \{F_2\}, \{F_3\}, \{F4\}, \{F_5\}, \{F_6\}, \{F_7\}\}$. For example, δ_{F_4} is the standard deviation of all data points in F_4, and μ_{F_4} is the mean of all data points in F_4. $F_4^{'}$ is a new set that includes the data points from F_4 and one data point from the test set. $\delta_{F_4'}$ is the standard deviation of all data points in $F_4^{'}$. $\mu_{F_4'}$ is the mean of all data points in $F_4^{'}$. In addition, $\delta_{F_4}^k (k = 1, 2, 3, 4)$ is δ_{F_4} for the k-th property. $\mu_{F_4}^k$, $\delta_{F_4'}^k$, and $\mu_{F_4'}^k$ have the same meaning. The steps involved in generating a complex-valued mass function are as follows:

step 1-1 The original dataset is randomly partitioned into training set, while the other data is allocated to test set.

step 1-2 Calculate the standard deviation($\delta_{F_p}^k$) and mean($\mu_{F_p}^k$) of training set associated with each proposition in each attribute.

step 1-3 Randomly select a data point from test set and add it to training set to form a new dataset. Calculate the standard deviation($\delta_{F_p'}^k$) and mean($\mu_{F_p'}^k$) of this new dataset associated with each proposition in each attribute.

step 1-4 Generate parameters related to the reliability of propositional support and propositional support.

$$\Delta\delta_{F_p}^k = |\delta_{F_p'}^k - \delta_{F_p}^k|, \Delta\mu_{F_p}^k = |\mu_{F_p'}^k - \mu_{F_p}^k|$$

Considering that when the phase angle describes the reliability information, its value range is $[0, \frac{\pi}{2}]$, so it is necessary to assign $\Delta\delta_{F_p}^k$ greater than $\frac{\pi}{2}$ to $\frac{\pi}{2}$.

step 1-5 Generate initial CVMF.

$$CM_k^o(F_p) = \left(\frac{1}{e^{\Delta\mu_{F_p}^k}}\right) e^{i\left(\Delta\delta_{F_p}^k\right)} \tag{16}$$

step 1-6 Normalize the initial CVMF to obtain the final CVMF.

$$CM_k(F_p) = \frac{CM_k^o(F_p)}{\sum_{p=1}^{1,2,\ldots,N} |CM_k^o(F_p)|} \tag{17}$$

4.1.2 Information fusion model based on CVBJ-SD

In this steps, CVBJ-SD is devised to measure the difference among the evidences. If the difference between one evidence and other evidences is small, indicating it has the less conflict with others and should obtain greater support. The specific method is as follows.

step 2-1 Through the application of the Equation 15, we can calculate the distance metric $CVBJ-SD_{ij}$ between the evidence bodies CM_i and $CM_j(1 \leq i, j \leq k, i \neq j)$. Subsequently, we construct CVBJ-SD matrix $DMM = (CVBJ-SD_{ij})_{k*k}$, as follows:

$$DMM = \begin{bmatrix} 0 & \ldots & CVBJ-SD_{1i} & \ldots & CVBJ-SD_{1k} \\ \vdots & \ldots & \vdots & \ldots & \vdots \\ CVBJ-SD_{i1} & \ldots & 0 & \ldots & CVBJ-SD_{ik} \\ \vdots & \ldots & \vdots & \ldots & \vdots \\ CVBJ-SD_{k1} & \ldots & CVBJ-SD_{ki} & \ldots & 0 \end{bmatrix} \tag{18}$$

step 2-2 The divergence between each evidence CM_i source and other evidence sources CM_j are calculated by

$$D_i = \sum_{j=1}^{k} CVBJ-SD_{ij}, 1 \leq i, j \leq k. \tag{19}$$

step 2-3 If D_i of evidence body CM_i is large, it indicates that evidence CM_i has a large difference with other evidences. In this case, evidence CM_i should be given a smaller credibility. Hence, the credibility cr_i of CM_i can be computed by

$$cr_i = e^{-D_i} \tag{20}$$

step 2-4 Based on credibility cr_i, the weight of evidence $\widetilde{w_i}$ is computed as follows.

$$\widetilde{w_i} = \frac{w_i}{\sum_{i=1}^{k} w_i}, \quad 1 \leq i \leq k \tag{21}$$

Hence, the vector of weight is $W = [\widetilde{w_1}, \widetilde{w_2}, \ldots, \widetilde{w_k}]$

step 2-5 Weight factor $\widetilde{w_i}(i = 1, 2, \ldots,)$ is used to correct the corresponding evidence CM_i, the weighted average evidence $WAE(CM)$ is computed by:

$$WAE(CM) = \sum_{i=1}^{k} (\widetilde{w_i} * CM_i), \quad 1 \leq i \leq k. \tag{22}$$

step 2-6 There are k evidences, so the weighted average evidence $WAE(CM)$ should be fused $k-1$ times by DCR to gain final fusion results.

$$F(WAE(CM)) = \Big(\big(\big((WAE(CM) \oplus WAE(CM))_1 \oplus WAE(CM)\big)_2 \oplus \cdots\big)_{k-2} \oplus WAE(CM)\Big)_{k-1} \tag{23}$$

where $F(WAE(CM))$ is the final fusion result.

4.2 Experimental results on real dataset

In this section, we have conducted our analyses using two datasets that are natively provided with Python: Iris and Wine, both accessible through the scikit-learn library.

In our experiment, the proportion of the training set increases sequentially, and remaining data is used as the test set. Conduct 100 random Monte Carlo experiments for each partition ratio.

4.2.1 Information fusion in Iris dataset

Taking the Iris dataset as an example, the specific steps for generating CVMFs are as follows:

step 1-1 We randomly select 70% of Iris as training set, and 30% as test set. The test point comes from the first data point of Vi.

step 1-2 The standard deviation (Table 1) and mean (Table 2) corresponding to the training set of each attribute.

Table 1 The mean corresponding to the training set of each attribute

attribute	$\mu^k_{F_1}$	$\mu^k_{F_2}$	$\mu^k_{F_3}$	$\mu^k_{F_4}$	$\mu^k_{F_5}$	$\mu^k_{F_6}$	$\mu^k_{F_7}$
SL(k=1)	4.9941	5.9219	6.6538	5.4439	5.8808	6.3239	5.8933
SW(k=2)	3.3824	2.7563	2.9872	3.0788	3.1712	2.8831	3.0448
PL(k=3)	1.4529	4.1969	5.5974	2.7833	3.6671	4.9662	3.8286
PW(k=4)	0.2324	1.3062	2.0308	0.7530	1.1932	1.7042	1.2276

Table 2 The standard deviation corresponding to the training set of each attribute

attribute	$\delta^k_{F_1}$	$\delta^k_{F_2}$	$\delta^k_{F_3}$	$\delta^k_{F_4}$	$\delta^k_{F_5}$	$\delta^k_{F_6}$	$\delta^k_{F_7}$
SL(k=1)	0.3548	0.5302	0.6527	0.6451	0.9857	0.7024	0.8727
SW(k=2)	0.3914	0.3399	0.3465	0.4826	0.4176	0.3623	0.4392
PL(k=3)	0.1419	0.4838	0.5604	1.4158	2.1098	0.8739	1.7960
PW(k=4)	0.0931	0.2045	0.2593	0.5593	0.9191	0.4310	0.7764

step 1-3 Add test points(SL:5.8; SW: 2.8; PL: 5.1; PW: 2.4), and calculate the standard deviation (Table 3) and mean (Table 4) corresponding to the new set of each attribute.

Table 3 The mean corresponding to the new training set of each attribute

attribute	$\mu^k_{F'_1}$	$\mu^k_{F'_2}$	$\mu^k_{F'_3}$	$\mu^k_{F'_4}$	$\mu^k_{F'_5}$	$\mu^k_{F'_6}$	$\mu^k_{F'_7}$
SL(k=1)	5.0171	5.9182	6.6325	5.4493	5.8797	6.3167	5.8925
SW(k=2)	3.3657	2.7576	2.9825	3.0746	3.1662	2.8819	3.0425
PL(k=3)	1.5571	4.2242	5.5850	2.8179	3.6865	4.9681	3.8406
PW(k=4)	0.2943	1.3394	2.0400	0.7776	1.2095	1.7139	1.2387

Table 4 The standard deviation corresponding to the new training set of each attribute

attribute	$\delta^k_{F'_1}$	$\delta^k_{F'_2}$	$\delta^k_{F'_3}$	$\delta^k_{F'_4}$	$\delta^k_{F'_5}$	$\delta^k_{F'_6}$	$\delta^k_{F'_7}$
SL(k=1)	0.3745	0.5225	0.6582	0.6417	0.9791	0.7002	0.8686
SW(k=2)	0.3978	0.3349	0.3434	0.4802	0.4170	0.3600	0.4378
PL(k=3)	0.6235	0.5009	0.5588	1.4330	2.1020	0.8679	1.7917
PW(k=4)	0.3726	0.2752	0.2625	0.5900	0.9234	0.4357	0.7810

step 1-4 Calculate the corresponding $\Delta\delta^k_{F_p}$(Table 5) and $\Delta\delta^k_{F_p}$(Table 6) for each attribute separately.

Table 5 The corresponding $\Delta\mu^k_{F_p}$ for each attribute

attribute	$\Delta\mu^k_{F_1}$	$\Delta\mu^k_{F_2}$	$\Delta\mu^k_{F_3}$	$\Delta\mu^k_{F_4}$	$\Delta\mu^k_{F_5}$	$\Delta\mu^k_{F_6}$	$\Delta\mu^k_{F_7}$
SL(k=1)	0.0230	0.0037	0.0213	0.0053	0.0011	0.0073	0.0009
SW(k=2)	0.0166	0.0013	0.0047	0.0042	0.0050	0.0012	0.0023
PL(k=3)	0.1042	0.0274	0.0124	0.0346	0.0194	0.0019	0.0120
PW(k=4)	0.0619	0.0331	0.0092	0.0246	0.0163	0.0097	0.0111

step 1-5 Generate the initial CVMFs, as shown in Table 7.

step 1-6 Normalize it to gain the final CVMFs, as shown in Table 8.

Next, we will use the final complex-valued mass functions as a numerical example to verify that our proposed fusion model has better fusion performance than directly using DCR.

Based on the method outlined in 4.1.2, the detailed steps are outlined below:

step 2-1 Construct $DMM = (CVBJ - SD_{ij})_{k*k}$:

$$DMM = \begin{bmatrix} 0 & 0.0521 & 0.1096 & 0.0943 \\ 0.0521 & 0 & 0.1089 & 0.0953 \\ 0.1096 & 0.1089 & 0 & 0.0671 \\ 0.0943 & 0.0953 & 0.0671 & 0 \end{bmatrix}$$

step 2-2 Calculate sum of the distance D_i between the evidence body CM_i and the other bodies of evidence :

$$D_1 = 0.2560, D_2 = 0.2563, D_3 = 0.2856, D_4 = 0.2567.$$

Table 6 The corresponding $\Delta\delta_{F_p}^k$ for each attribute

attribute	$\Delta\delta_{F_1}^k$	$\Delta\delta_{F_2}^k$	$\Delta\delta_{F_3}^k$	$\Delta\delta_{F_4}^k$	$\Delta\delta_{F_5}^k$	$\Delta\delta_{F_6}^k$	$\Delta\delta_{F_7}^k$
SL(k=1)	0.0198	0.0077	0.0054	0.0034	0.0066	0.0022	0.0041
SW(k=2)	0.0064	0.0051	0.0031	0.0024	0.0006	0.0024	0.0014
PL(k=3)	0.4816	0.0171	0.0016	0.0172	0.0078	0.0059	0.0043
PW(k=4)	0.2795	0.0706	0.0031	0.0306	0.0043	0.0047	0.0046

step 2-3 Calculate weight w_i of CM_i:

$$w_1 = 0.7741, w_2 = 0.7739, w_3 = 0.7516, w_4 = 0.7736.$$

step 2-4 Normalize to obtain the final weight $\widetilde{w_i}$ of CM_i:

$$\widetilde{w_1} = 0.2519, \widetilde{w_2} = 0.2518, \widetilde{w_3} = 0.2446, \widetilde{w_4} = 0.2517.$$

step 2-5 Calculate the weighted average evidence $WAE(CM)$:

$$\begin{aligned}
&CM(\text{Se}) = 0.1229 + 0.0056j,\\
&CM(\text{Ve}) = 0.1438 + 0.0024j,\\
&CM(\text{Vi}) = 0.1472 + 0.0017j,\\
&CM(\text{Se, Ve}) = 0.1455 + 0.0025j,\\
&CM(\text{Se, Vi}) = 0.1468 + 0.0016j,\\
&CM(\text{Ve, Vi}) = 0.1469 + 0.0007j,\\
&CM(\text{Se, Ve, Vi}) = 0.1469 + 0.0010j.
\end{aligned}$$

step 2-6 Calculate the final combination result of multi-evidences. Here, $k = 4$, we need to fuse 3 times through the complex-valued DCR:

$$\begin{aligned}
&CM(\text{Se}) = 0.2733 + 0.0082j,\\
&CM(\text{Ve}) = 0.3238 - 0.0016j,\\
&CM(\text{Vi}) = 0.3349 - 0.0055j,\\
&CM(\text{Se, Ve}) = 0.0219 - 0.0000j,\\
&CM(\text{Se, Vi}) = 0.0223 - 0.0004j,\\
&CM(\text{Ve, Vi}) = 0.0223 - 0.0003j,\\
&CM(\text{Se, Ve, Vi}) = 0.0015 - 0.0000j.
\end{aligned}$$

Subsequently, the CM is converted using the complex Pignistic probability transformation, resulting in the following:

$$\text{Bet}^C(\text{Se}) = 0.2960, \quad \text{Bet}^C(\text{Ve}) = 0.3464, \quad \text{Bet}^C(\text{Vi}) = 0.3576.$$

Table 7 The initial complex-valued mass functions $CM_k^o(F_p)$

attribute	$CM_k^o(F_1)$	$CM_k^o(F_2)$	$CM_k^o(F_3)$	$CM_k^o(F_4)$	$CM_k^o(F_5)$	$CM_k^o(F_6)$	$CM_k^o(F_7)$
SL(k=1)	0.9801+0.0226i	0.9923+0.0037i	0.9944+0.0212i	0.9966+0.0053i	0.9934+0.0011i	0.9978+0.0073i	0.9959+0.0009i
SW(k=2)	0.9935+0.0165i	0.9950+0.0013i	0.9969+0.0047i	0.9976+0.0042i	0.9994+0.0050i	0.9976+0.0012i	0.9986+0.0023i
PL(k=3)	0.6145+0.0643i	0.9826+0.0269i	0.9983+0.0124i	0.9824+0.0340i	0.9921+0.0192i	0.9941+0.0018i	0.9957+0.0119i
PW(k=4)	0.7547+0.0468i	0.9313+0.0309i	0.9968+0.0092i	0.9695+0.0238i	0.9955+0.0162i	0.9953+0.0096i	0.9954+0.0110i

Table 8 The final complex-valued mass functions $CM_k(F_p)$

attribute	$CM_k(F_1)$	$CM_k(F_2)$	$CM_k(F_3)$	$CM_k(F_4)$	$CM_k(F_5)$	$CM_k(F_6)$	$CM_k(F_7)$
SL(k=1)	0.1410+0.0032i	0.1428+0.0005i	0.1431+0.0031i	0.1434+0.0008i	0.1429+0.0002i	0.1435+0.0010i	0.1433+0.0001i
SW(k=2)	0.1424+0.0024i	0.1426+0.0002i	0.1428+0.0007i	0.1429+0.0006i	0.1432+0.0007i	0.1430+0.0002i	0.1431+0.0003i
PL(k=3)	0.0936+0.0098i	0.1497+0.0041i	0.1521+0.0019i	0.1497+0.0052i	0.1518+0.0029i	0.1514+0.0003i	0.1517+0.0018i
PW(k=4)	0.1136+0.0070i	0.1402+0.0046i	0.1504+0.0014i	0.1460+0.0036i	0.1499+0.0024i	0.1499+0.0014i	0.1499+0.0017i

Among them, Vi has the highest probability, and in the experiment, the testing point also come from Vi, and the combination results are in line with intuition.When this situation occurs, we consider the classification to be correct.

4.2.2 Discussion and analysis

In this part, we compare the average fusion accuracy achieved by two distinct methods: between directly using complex-valued DCR and using proposed method, across 100 random Monte Carlo experiments. Taking the Iris dataset as an example, Figure 5 illustrates average fusion accuracy as the training set ratio varies from 0.2 to 0.9. Figure 6 illustrates average fusion accuracy in 100 experiments when the training set ratio is 0.5. The same applies to the Wine dataset as shown in Figure 7 and Figure 8.

To sum up, it can be seen that compared to directly using the complex-valued DCR, our proposed method can achieve higher average fusion accuracy regardless of how the training set changes. Especially on the Wine dataset, the average fusion accuracy has seen a significant improvement.

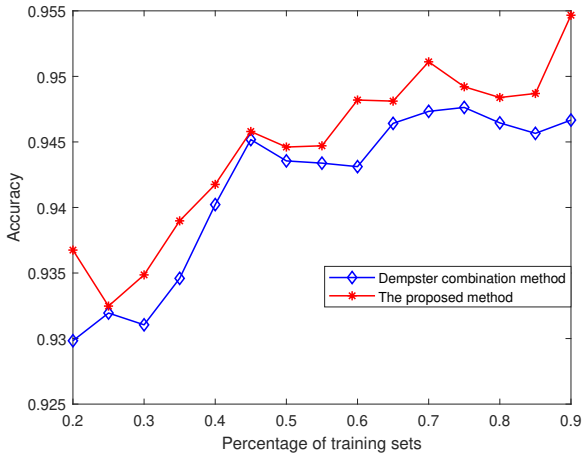

Fig. 5 This is the average fusion accuracy as the training set ratio varies from 0.2 to 0.9 in Iris dataset

5 Conclusion

This paper introduces a multi-sensor data fusion strategy that utilizes complex-valued belief Jensen-Shannon divergence to quantify information difference and offer a more precise information fusion approach for decision systems. Our proposed method consists of three primary steps. Initially, a novel divergence was introduced to quantify the distance between the evidence bodies. Subsequently, the weight of each evidence body was computed based on its distance from the others. This weight was then utilized to derive the weighted average evidence. In the third step, DCR was applied

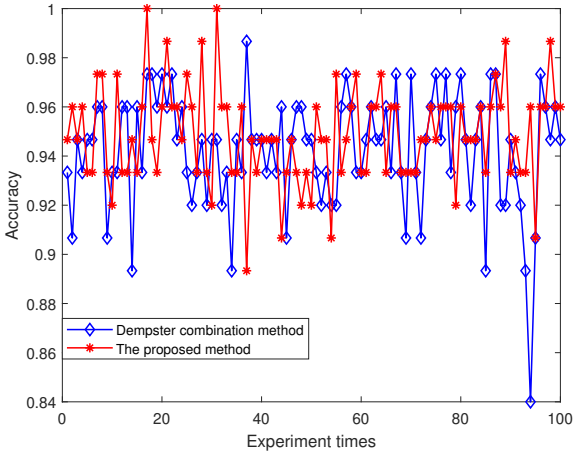

Fig. 6 This is the average fusion accuracy in 100 experiments when the training set ratio is 0.5 in Iris dataset

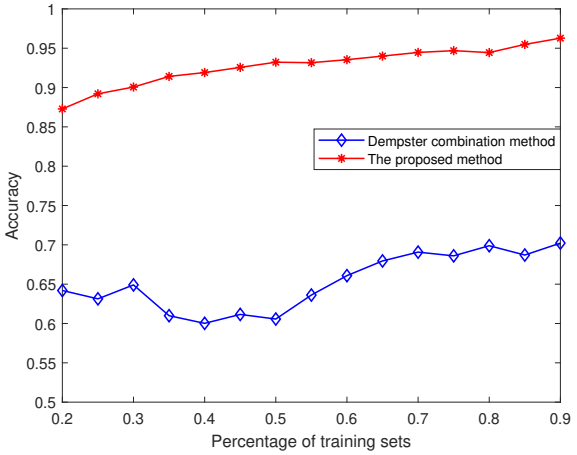

Fig. 7 This is the average fusion accuracy as the training set ratio varies from 0.2 to 0.9 in Wine dataset

to fuse information. Ultimately, real world data sets are illustrates that the proposed method can improve the accuracy of fusion results.

6 Acknowledge

The work is partially supported by the National Natural Science Foundation of China (Grant No. 62303382, 62403388), and by Qin Chuangyuan high-level innovation and entrepreneurship talent program of Shaanxi(Grant No.QCYRCXM-2023-108), and by Guangdong Basic and Applied Basic Research Foundation(Grant No.

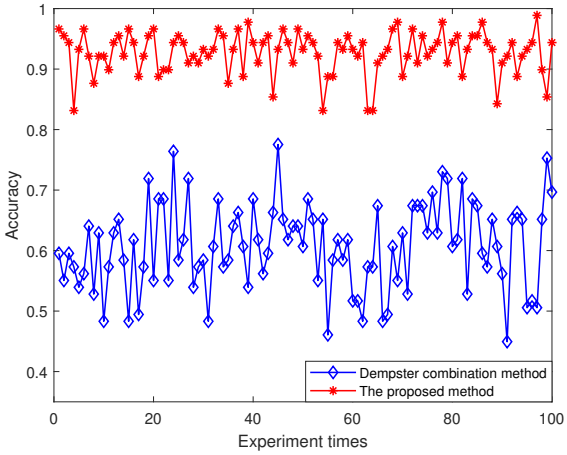

Fig. 8 This is the average fusion accuracy in 100 experiments when the training set ratio is 0.5 in Wine dataset

2023A1515110784), Shaanxi Fundamental Science Research Project for Mathematics and Physics (Grant No. 23JSQ034), and by 2024 College Student Innovation Training Program Project(Grant No. 202410712230).

7 Declarations

Data availability:

No data was used for the research described in the article.

Conflicts of interest:

The authors declare no conflict of interest.

Author contributions:

Mengzhuo Zhang: Conceptualization, Methodology, Writing–original draft, Writing – review & editing.

Yifan Sun: Formal analysis, Investigation, Writing.

Xiaozhuan Gao: Formal analysis, Investigation, Writing–review & editing.

Lipeng Pan: Resources, Supervision, Funding acquisition, Writing–review & editing.

References

[1] Vandecasteele, F., Merci, B., Verstockt, S.: Reasoning on multi-sensor geographic smoke spread data for fire development and risk analysis. Fire Safety Journal **86**, 65–74 (2016)

[2] Fei, L., Li, T., Ding, W.: Dempster–shafer theory-based information fusion for natural disaster emergency management: A systematic literature review. Information Fusion, 102585 (2024)

[3] Kibrete, F., Woldemichael, D.E., Gebremedhen, H.S.: Multi-sensor data fusion in intelligent fault diagnosis of rotating machines: A comprehensive review. Measurement, 114658 (2024)

[4] Muzammal, M., Talat, R., Sodhro, A.H., Pirbhulal, S.: A multi-sensor data fusion enabled ensemble approach for medical data from body sensor networks. Information Fusion **53**, 155–164 (2020)

[5] Elamin, A., El-Rabbany, A.: Uav-based multi-sensor data fusion for urban land cover mapping using a deep convolutional neural network. Remote sensing **14**(17), 4298 (2022)

[6] Kumar, K.K., Ramaraj, E., Geetha, P.: Multi-sensor data fusion for an efficient object tracking in internet of things (iot). Applied Nanoscience **13**(2), 1355–1365 (2023)

[7] Xu, X., Guo, H., Zhang, Z., Shi, P., Huang, W., Li, X., Brunauer, G.: Fault diagnosis method via one vs rest evidence classifier considering imprecise feature samples. Applied Soft Computing **161**, 111761 (2024)

[8] Deng, J., Deng, Y., Yang, J.-B.: Random permutation set reasoning. IEEE Transactions on Pattern Analysis and Machine Intelligence **46**, 10246–10258 (2024)

[9] Zhang, Z., Liu, Z., Ning, L., Martin, A., Xiong, J.: Representation of imprecision in deep neural networks for image classification. IEEE Transactions on Neural Networks and Learning Systems, 10–110920233329712 (2023)

[10] Lee, P.M.: Probability theory. Bulletin of the London Mathematical Society **12**, 318–319 (1980)

[11] Walczak, B., Massart, D.L.: Rough sets theory. Chemometrics and Intelligent Laboratory Systems **47**, 1–16 (1999)

[12] Zadeh, L.A.: Fuzzy sets. Information and Control **8**, 338–353 (1965)

[13] Dempster, A.P.: In: Yager, R.R., Liu, L. (eds.) Upper and Lower Probabilities Induced by a Multivalued Mapping, pp. 57–72. Springer, Berlin, Heidelberg (2008). https://doi.org/10.1007/978-3-540-44792-4_3

[14] Shafer, G.: A Mathematical Theory of Evidence. Princeton University Press, Princeton (1976). https://doi.org/10.1515/9780691214696

[15] Deng, Y.: Random permutation set. International Journal of Computers Communications & Control **17**(1), 4542 (2022)

[16] Zadeh, L.A.: A note on z-numbers. Information Sciences **181**, 2923–2932 (2011)

[17] Pan, L., Deng, Y.: A new complex evidence theory. Information Sciences **608**, 251–261 (2022)

[18] Zhao, J., Wang, Z., Yu, D., Cao, J., Cheong, K.H.: Swarm intelligence for protecting sensitive identities in complex networks. Chaos, Solitons & Fractals **182**, 114831 (2024)

[19] Wang, H., Feng, Y., Fei, L.: Uncertain linear programming with cloud set constraints integrating fuzziness and randomness. Applied Soft Computing **151**, 111157 (2024)

[20] Joseph, C.W., Kathrine, G.J.W., Vimal, S., Sumathi, S., Pelusi, D., Valencia, X.P.B., Verdú, E.: Improved optimizer with deep learning model for emotion detection and classification. Mathematical biosciences and engineering: MBE **21**(7), 6631–6657 (2024)

[21] Zhao, J., Cheong, K.H.: Early identification of diffusion source in complex networks with evidence theory. Information Sciences **642**, 119061 (2023)

[22] Sezer, S.I., Akyuz, E., Arslan, O.: An extended heart dempster–shafer evidence theory approach to assess human reliability for the gas freeing process on chemical tankers. Reliability Engineering & System Safety **220**, 108275 (2022)

[23] Zhang, H., Chang, Y., Zhang, Y., Kang, B.: Evaluate the competence of fuzzy preference using statistical conflict in the frame of ds evidence theory. Applied Soft Computing **164**, 112017 (2024)

[24] Bisht, K., Kumar, A.: A portfolio construction model based on sector analysis using dempster-shafer evidence theory and granger causal network: An application to national stock exchange of india. Expert Systems with Applications **215**, 119434 (2023)

[25] Zhou, Q., Pedrycz, W., Deng, Y.: Order-2 probabilistic information fusion on random permutation set. IEEE Transactions on Knowledge & Data Engineering (01), 1–14 (2024)

[26] Turhan, H.I., Tanaydin, T.: A novel optimization-based combination rule for dempster-shafer theory. In: International Conference on Belief Functions, pp. 180–188 (2024). Springer

[27] Zhou, Q., Deng, Y., Yager, R.R.: Cd-bft: Canonical decomposition-based belief functions transformation in possibility theory. IEEE Transactions on Cybernetics **54**, 611–623 (2023)

[28] Zhang, S., Han, D., Dezert, J., Yang, Y.: Weighted self-paced learning with belief functions. Expert Systems with Applications **255**, 124535 (2024)

[29] Tian, H., Zhang, Z., Ding, W.: Incomplete data transfer calibration classification. IEEE Transactions on Emerging Topics in Computational Intelligence, 1–13 (2024)

[30] Belmahdi, F., Lazri, M., Ouallouche, F., Labadi, K., Absi, R., Ameur, S.: Application of dempster-shafer theory for optimization of precipitation classification and estimation results from remote sensing data using machine learning. Remote Sensing Applications: Society and Environment **29**, 100906 (2023)

[31] Zhang, Z., Zhang, Y., Tian, H., Martin, A., Liu, Z., Ding, W.: A survey of evidential clustering: Definitions, methods, and applications. Information Fusion **115**, 102736 (2025)

[32] Dick, S., Yager, R.R., Yazdanbakhsh, O.: On pythagorean and complex fuzzy set operations. IEEE Transactions on Fuzzy Systems **24**(5), 1009–1021 (2015)

[33] Xue, S., Deng, X., Jiang, W.: An improved quantum combination method of mass functions based on supervised learning. Information Sciences **652**, 119757 (2024)

[34] Ashraf, S., Garg, H., Kousar, M.: An industrial disaster emergency decision-making based on china's tianjin city port explosion under complex probabilistic hesitant fuzzy soft environment. Engineering Applications of Artificial Intelligence **123**, 106400 (2023)

[35] Ramot, D., Milo, R., Friedman, M., Kandel, A.: Complex fuzzy sets. IEEE transactions on fuzzy systems **10**(2), 171–186 (2002)

[36] Garg, H., Rani, D.: Novel aggregation operators and ranking method for complex intuitionistic fuzzy sets and their applications to decision-making process. Artificial Intelligence Review **53**, 3595–3620 (2020)

[37] Zhang, S., Xiao, F.: A tfn-based uncertainty modeling method in complex evidence theory for decision making. Information Sciences **619**, 193–207 (2023)

[38] Xiao, F., Pedrycz, W.: Negation of the quantum mass function for multisource quantum information fusion with its application to pattern classification. IEEE Transactions on Pattern Analysis and Machine Intelligence **45**, 2054–2070 (2023)

[39] Pan, L., Deng, Y., Pelusi, D.: A similarity measure of complex-valued evidence theory for multi-source information fusion. Information Sciences **647**, 119416 (2023)

[40] Xia, R., Xiao, F.: A complex plausibility belief jensen–shannon divergence with its application in multi-source information fusion. Engineering Applications of Artificial Intelligence **137**, 109056 (2024)

[41] Rani, P., Mishra, A.R., Pardasani, K.R., Mardani, A., Liao, H., Streimikiene, D.:

A novel vikor approach based on entropy and divergence measures of pythagorean fuzzy sets to evaluate renewable energy technologies in india. Journal of Cleaner Production **238**, 117936 (2019)

[42] Hua, Z., Jing, X.: An improved belief hellinger divergence for dempster-shafer theory and its application in multi-source information fusion. Applied Intelligence **53**(14), 17965–17984 (2023)

[43] Shenoy, P.P.: Mutual information and kullback-leibler divergence in the dempster-shafer theory. In: International Conference on Belief Functions, pp. 225–233 (2024). Springer

[44] Pan, L., Deng, Y.: Complex-valued deng entropy. Applied Intelligence **53**, 21201–21210 (2023)

[45] Xiao, F.: Multi-sensor data fusion based on the belief divergence measure of evidences and the belief entropy. Information Fusion **46**, 23–32 (2019)

[46] Garg, H., Rani, D.: Novel exponential divergence measure of complex intuitionistic fuzzy sets with an application to the decision-making process. Scientia Iranica **28**(4), 2439–2456 (2021)

[47] Zhang, L., Xiao, F.: Belief re´ nyi divergence of divergence and its application in time series classification. IEEE Transactions on Knowledge and Data Engineering **36**, 3670–3681 (2024)

[48] Liu, R., Li, Z., Deng, Y.: Performance evaluation of information fusion systems based on belief entropy. Engineering Applications of Artificial Intelligence **127**, 107262 (2024)